Atom-Resolved Surface Structures and Molecular Adsorption on TiO_2(001) Investigated by Scanning Tunneling Microscopy

Ryugo Tero, Ken-ichi Fukui,† and Yasuhiro Iwasawa*

Department of Chemistry, Graduate School of Science, The University of Tokyo, Hongo, Bunkyo-ku, Tokyo 113-0033, Japan

Received: October 10, 2002; In Final Form: January 7, 2003

Well-ordered surface structure was prepared on a rutile TiO_2(001) surface and investigated on the atomic scale by scanning tunneling microscopy (STM). The surface had a latticework-like structure with rows running along the [110] and [1$\bar{1}$0] directions. Each row consisted of narrow terraces separated by single-height steps on their slopes at both sides. An added-row structural model that consists of Ti_7O_{12} suboxide row added on each narrow terrace of a {114}-microfacet structure was proposed on the basis of atom-resolved STM images as well as local coordination considerations. The added row had 4-fold coordinated and 5-fold coordinated Ti atoms, each of which was observed as a bright spot in STM images. Formic acid molecules adsorbed on both Ti sites, while methanol adsorbed preferentially on the 4-fold coordinated Ti atoms, which may support the validity of the structural model. The latticework structure was proved to be stable against thermal reactions of formic acid and methanol.

1. Introduction

Metal oxides are key materials for many industrial technologies such as catalysts, gas sensors, semiconductor devices, and so forth.[1,2] Among a variety of oxides, the (110) surface of rutile-type TiO_2 has been most extensively studied as a representative oxide surface.[3,4] A TiO_2 (110) surface is the most stable among the low-index planes of rutile-type TiO_2. The surface structure of TiO_2(110) is almost identical to bulk termination as proved by experimental techniques[5,6] and theoretical calculations.[7,8] One-dimensional rows of 5-fold coordinated Ti atoms and bridged O atoms along the [001] direction are arranged alternately. Each Ti atom and each O atom in the rows has been clearly observed by scanning tunneling microscopy (STM)[4,9] and noncontact atomic force microscopy (NC-AFM),[10] respectively. Previous STM measurements of the TiO_2(110)-(1 × 1) surface during the catalytic reaction of formic acid[11,12] and the surface reaction of acetic acid[13] have shown that the surface structure is stable during the reaction. However, the surface structures have drastically changed by annealing the surface in the presence of oxygen atmosphere because of the reaction of oxygen with Ti^{n+} cations that diffused to the surface from interstitial of bulk TiO_2, forming the added layer of TiO_x ($x = 1-2$) depending on the conditions.[14−16]

In contrast, there has been rather limited number of studies reported on TiO_2(001). Figure 1 shows a bulk-terminated structure of TiO_2(001) with a half-height step (0.15 nm). Cleaving between adjacent charge-neutral planes parallel to the (001) plane would produce two equivalent terraces where O−Ti−O rows are rotated by 90° from each other. All the exposed Ti atoms take 4-fold coordination, doubly unsaturated compared with Ti atoms in the bulk. This surface is nonpolar but unstable because of low ligand coordination. Theoretical calculations have revealed that the (001) termination has significantly higher surface energy than the (110) and the (100) termination.[7,8] Surface reconstruction was suggested to occur to stabilize the surface. In fact, two ordered phases have been observed by low-energy electron diffraction (LEED) on TiO_2-(001) depending on annealing temperature.[17,18] The lower- and the higher-temperature phases were assigned as {011}-facet and {114}-faceted structures, respectively, on the basis of kinematic LEED analysis.[18] To date, some structural analyses of TiO_2-(001) surfaces by scanning probe microscopies (SPM) have been reported. In the first STM observation of TiO_2(001), faceted structures which included mainly (011) planes were observed after annealing at 783 K for 30 min to 2 h.[19] Following STM and AFM, studies on TiO_2(001) also showed faceted or disordered reconstruction after thermal treatments under UHV.[20−22] Recently, Nörenberg et al. reported another phase of TiO_2(001), which appeared under nonequilibrium conditions.[23] Networklike structure with ($7\sqrt{2} \times \sqrt{2}$) periodicity

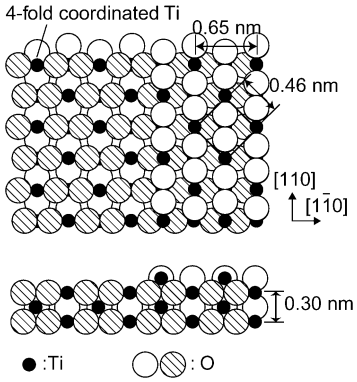

Figure 1. Bulk-terminated structural model of a rutile-type TiO_2(001) surface which includes a half-height step along the [110] direction. Filled circles represent Ti atoms. Empty and meshed larger circles represent oxygen atoms.

* To whom correspondence should be addressed. Fax: +81-3-5800-6892; e-mail: iwasawa@chem.s.u-tokyo.ac.jp.

† Present address: Department of Chemistry, Graduate School of Science and Engineering, Tokyo Institute of Technology, Ookayama, Meguro-ku, Tokyo 152-8550, Japan.

10.1021/jp0222090 CCC: $25.00
Published on Web 03/19/2003

was observed after annealing the sample to temperatures higher than 1473 K with heating and cooling rate of 100 K/s.

Barteau and co-workers[24−27] have studied surface reactions on TiO_2(001) by temperature-programmed desorption (TPD) for two ordered surfaces reported by the LEED study.[17,18] Chemical activity of the surfaces was extremely different among an Ar^+-sputtered surface, a lower-temperature phase, and a higher-temperature phase. Especially on the higher-temperature phase, which was assigned to {114}-faceted surface,[18] products of dimerization reaction were detected, such as dimethyl ether and acetone from methanol and acetic acid, respectively. These products were not detected on the lower-temperature phase as well as on the most stable TiO_2(110) surface. The active sites of the dimerization reactions were proposed to be 4-fold coordinated Ti atoms remaining on the faceted surface. To elucidate the reason for such unique chemical activities, information of atomic-scale structure is inevitable to be obtained. However, investigation on atomic-scale structures of ordered TiO_2(001) surfaces has not been so successful, partially because it is difficult to prepare a homogeneous structure on TiO_2(001), which is tolerable for precise measurements with high spatial resolution by SPM.

In the present study, we have succeeded in preparing the homogeneous surface on TiO_2(001), which corresponds to the higher temperature phase reported by previous LEED studies, and in imaging the surface structure on the atomic scale by STM for the first time. The surface was not a previously proposed macrofaceted structure but an atomically ordered latticework-like structure that consisted of wide rows running along the [110] and [1$\bar{1}$0] directions with steps and narrow terraces on their slopes. We propose a new structural model on the basis of atom-resolved STM images and adsorption of formic acid and methanol as probe molecules on the surface. The latticework structure was proved to be relatively stable against reactions of adsorbed formic acid and methanol.

2. Experimental Section

The experiments were performed in an ultrahigh vacuum (UHV) STM (JEOL JSTM 4500VT) equipped with an Ar^+ ion gun and a LEED optics. The base pressure was 1×10^{-8} Pa. A polished TiO_2(001) wafer of $6.5 \times 1 \times 0.25$ mm^3 (Earth Chemical) was used after deposition of Ni film on the rear side of the sample to resistively heat the sample on a sample holder. Heating rate and cooling rate was controlled to be 7−10 K s^{-1}. The TiO_2(001) surface was cleaned with cycles of Ar^+ ion sputtering (3 keV for 2 min) and annealing under UHV at ca. 900 K. Constant current topographies (CCT) and variable current images (VCI) (mapping of logarithm of the tunneling current at constant height over the sample) were obtained at room temperature (RT) with electrochemically etched W tips. Formic acid (Wako, 96% purity, most of the contaminant is water) and methanol (Wako, contamination less than detection limit) used in this study were purified by repeated freeze−pump−thaw cycles and introduced into the chamber by backfilling. The surface temperature of the crystal was monitored by an infrared radiation thermometer.

3. Results

Figure 2 shows a wide range STM image (100×100 nm^2) after annealing an Ar^+-ion-sputtered TiO_2(001) surface at 1050 K for 300 s with the heating and cooling rate of ca. 7 K s^{-1}. This surface had a latticework-like structure that consisted of wide rows running along the [110] and [1$\bar{1}$0] directions, which were crossed and piled up. We confirmed by STM that almost

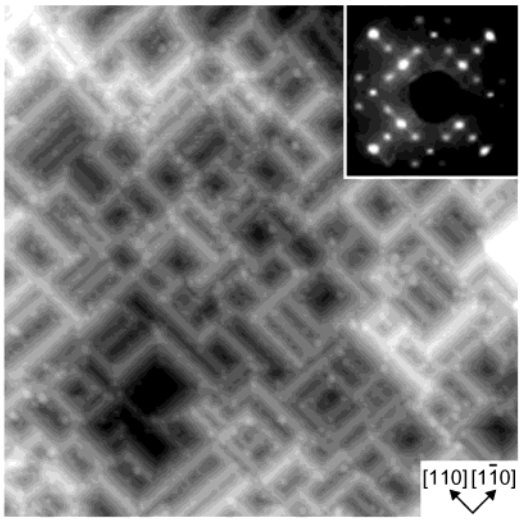

Figure 2. Constant current topography (CCT) image (100×100 nm^2, V_s: +2.0 V, I_t: 0.02 nA) of a TiO_2(001) surface after annealing an Ar^+-ion-sputtered surface at 1050 K for 5 min. The inset shows a simultaneously obtained LEED pattern at a primary energy of 43 eV.

the whole surface was covered with this rather flat structure by careful control of heating and cooling procedure. It was also supported from a good contrast LEED pattern simultaneously obtained from the surface. When annealing temperature was as low as 970 K, a large scale hill-like structure was observed by STM as briefly reported previously.[28] The hill-like structure was inhomogeneous on the whole surface and did not develop to flat surface at the temperature. At annealing temperatures above 1150 K, particle-like protrusions that had wide distribution 1.5−16 nm in diameter covered the surface and did not convert to a flat surface by further heat treatment unless the surface was sputtered with Ar^+ ion.[28]

The LEED pattern shown in the inset of Figure 2 is probably identical to that of the previously reported higher-temperature phase.[18] Annealing temperature and the primary electron energy to obtain a good contrast pattern were almost identical to the previous studies.[18,25] Firment considered that the higher-temperature phase was faceted because the subspots did not converse to the specular spots when the primary electron energy changed and assigned it to a {114}-faceted structure.[18] In the present study, subspots also moved as a function of electron energy as was expected from the {114}-faceted structure. However, the corresponding surface observed by STM (Figure 2) was rather flat and did not seem to hold the character of typical macrofaceted structure.

Figure 3 shows atom-resolved STM images of the latticework structure on TiO_2(001) shown in Figure 2. They included some crossing points of the rows, each of which was imaged as a wide row in Figure 2. Figure 3a clearly reveals that each wide row consists of narrow terraces separated with steps at both sides of its slope, forming a structurelike "bleachers". As shown by a magnified image at the topmost terrace of the row (Figure 3b), three bright spots, which were lined perpendicular to the row axis, were arranged with a regular interval of 0.65 nm along the row axis. Among the three bright spots, the center one (denoted by a filled circle) was higher than the side ones (denoted by open circles) by 0.05 nm in topography. Hereinafter we call them a "center-bright spot" and "side-bright spots", respectively. Distance between the side-bright spots and the center-bright spot was 0.50 ± 0.04 nm. The variable-current image in Figure 3c and its magnified image in Figure 3d show that the whole narrow terraces of the stepped wide row consist

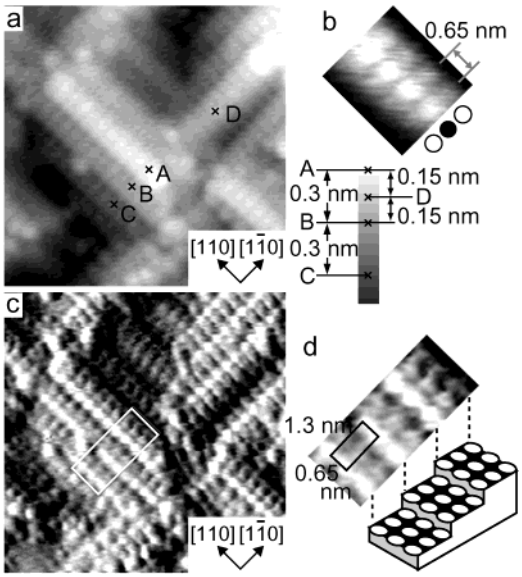

Figure 3. Atom-resolved STM images of a latticework structure on TiO_2(001): (a) a CCT image (15 × 15 nm^2, V_s: +2.0 V, I_t: 0.20 nA), (b) a magnified image (2.6 × 2.3 nm^2, V_s: +2.0 V, I_t: 0.14 nA) of the topmost terrace in (a), and (c) a variable current STM image (15 × 15 nm^2, V_s: +2.0 V, I_t: ∼0.15 nA) at the same area as (a). (d) A magnified image of the rectangular area in (c) and a schematic drawing showing the relative position of the bright spots.

of the bright spots with the same periodicity as that of the topmost terrace. Thus, the wide row was an atomically ordered structure with a unit cell of 1.30 × 0.65 nm^2 on the projection to the (001) surface as shown in Figure 3d. The unit cell dimension was the same as that of the {114}-faceted structure. The height difference of the narrow terraces A, B, and C in Figure 3a was 0.30 nm, which corresponded to the single-step height of the TiO_2(001) surface. The average slope of the wide row was calculated to be inclined from the (001) surface by 13°. Thus, the average planes at both sides of the wide row corresponded to the {114} plane. The height difference between the terraces of the crossing rows (A and D or B and D in Figure 3a) was 0.15 nm, half of a single-step height. The structure of the wide row was equivalent regardless of the row direction. As shown in Figure 1, TiO_2(001) consists of planes with one-dimensional O−Ti−O rows, which alternately rotate by 90° by each other. Therefore, the latticework structure holds the symmetry of the bulk-terminated TiO_2(001) structure.

In some cases, the unit cell self-assembled to form rather wide {114} surfaces. A pyramidal structure, which consisted of four equivalent {114} surfaces, was also observed (Figure 4). An atom-resolved STM image in Figure 4 clearly indicated that it consisted of the equivalent unit cell to the latticework structure (Figure 3). Formation of the pyramidal structure indicates that the connection of the stepped wide row along the [110] and [1$\bar{1}$0] directions is not accompanied by large stress.

STM observations of adsorption behavior of molecules sometimes help to characterize a surface cation sites of oxides.[29] Formic acid dissociates on TiO_2 surfaces to give formate anion at RT:[12]

$$HCOOH(g) + O^{2-}(s) \rightarrow HCOO^{-}(a) + OH^{-}(a) \quad (1)$$

where $O^{2-}(s)$ represents oxygen anion at the surface. Selective adsorption of formate ions on Ti cation sites has been used to identify the exposed Ti cation sites on TiO_2 surfaces by STM.[30−33] Figure 5a shows an STM image of the latticework structure after exposure to 12 L (1 L = 1.33 × 10^{-4} Pa s) of

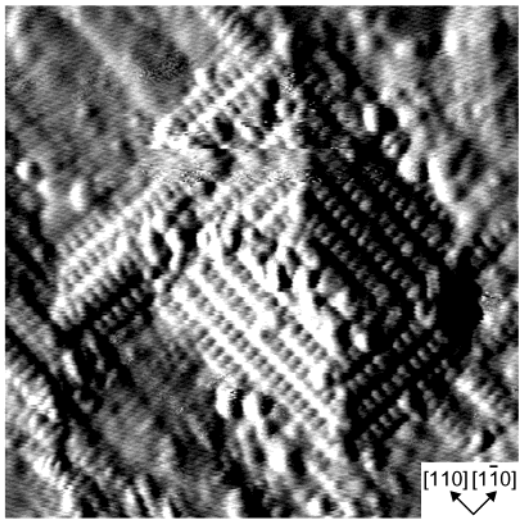

Figure 4. A variable current STM image (27 × 27 nm^2, V_s: +2.0 V, I_t: ∼0.1 nA) of a pyramidal structure on TiO_2(001) after annealing an Ar^+-ion-sputtered surface at 1050 K for 5 min.

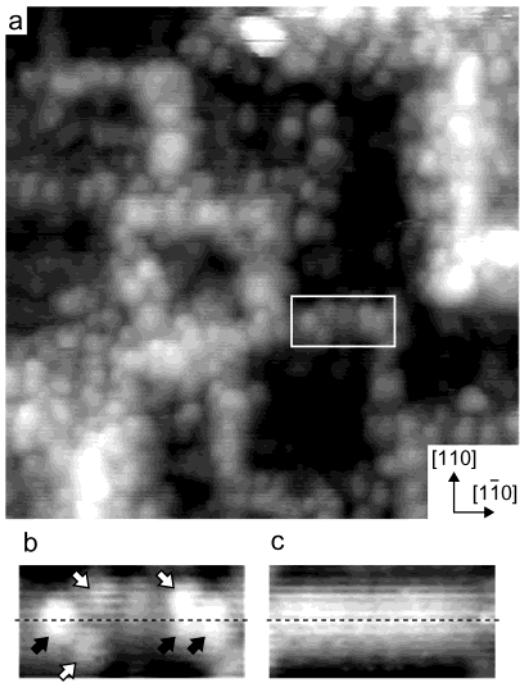

Figure 5. (a) CCT (30 × 30 nm^2, V_s: +2.0 V, I_t: 0.2 nA) of a latticework structure on TiO_2(001) after exposure to 12 L of formic acid at RT. Each adsorbed formate ion was imaged as a bright protrusion on the row structure. (b) Magnified image of the rectangular area in (a). (c) CCT (V_s: +1.0 V, I_t: 0.50 nA) at the same area as (b) before exposure to formic acid as a reference. The image contrast in (c) is much higher than that in (b) to enhance the contrast difference of top narrow terrace. Periodicity of 0.65 nm along the row axis can be confirmed. Dotted lines in (b) and (c) indicate the row of center-bright spots at the top of the row. Black and white arrows in (b) indicate adsorbed formates on center-bright spots and side-bright spots, respectively.

formic acid at RT. By comparing the image with that obtained before exposure at the same area, new bright features were observed on the narrow terraces and their density increased with exposure. Figure 5b is a magnified STM image of a part of a topmost terrace of a stepped wide row surrounded by a rectangle in Figure 5a, and Figure 5c is that of the same region before exposure to formic acid vapor. The newly formed bright spots had a corrugation of approximately 0.17 ± 0.02 nm by line profile analyses along the row−axis. It indicates that a single

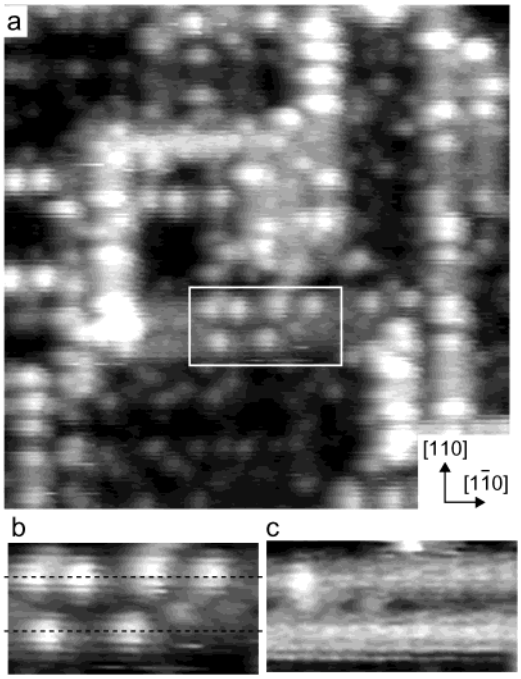

Figure 6. (a) CCT (24 × 24 nm^2, V_s: +1.2 V, I_t: 0.02 nA) of a latticework structure on TiO_2(001) after exposure to 3.0 L of methanol at RT. Each adsorbed methoxy species was imaged as a bright protrusion on the row structure. (b) Magnified image of the rectangular area in (a). (c) CCT (V_s: +2.0 V, I_t: 0.06 nA) at the same area as (b) before exposure to methanol as a reference. The image contrast in (c) is much higher than that in (b) to enhance the contrast difference of top narrow terrace. The bright spots, which may be structural defects, in (c) are much lower than methoxy and cannot be recognized in (b). Dotted lines in (b) and (c) indicate the rows of center-bright spots at the top terraces of two parallel rows. The two narrow terraces were the same height and separated by a narrow terrace which was 0.30 nm lower than them.

adsorbate was imaged. The corrugation of the bright spot was close to that of formates (0.14 nm) on exposed Ti cations at TiO_2(110) with a similar tunneling condition.[30,31] Thus, they can be assigned to formate ions formed by eq 1. Although bright spots of the substrate were not resolved in Figure 5b and 5c as in Figures 3 and 4, the images indicate that formate ions adsorbed on the sites expected for both center-bright spots (indicated by black arrows in Figure 5b) and side-bright spots (indicated by white arrows in Figure 5b) without any preference. Formate ions did not form any ordered structure on the surface even after further exposure. Surface hydroxyls, which were simultaneously formed with formates (eq 1), were not observed by STM as in the case of TiO_2(110).[30,31] Käckell and Terakura have revealed that a surface formate on TiO_2(110) surface is stabilized forming a complex with neighboring hydroxyl species.[34] It may be the reason we could not image hydroxyl species by STM. In a recent study on formic acid adsorption on anatase TiO_2(001)−(1 × 4) surface, hydroxyl species were recognized neither by STM nor NC-AFM, although surface formate was clearly observed.[33]

Methanol is known as a much weaker Brønsted acid than formic acid. Adsorption of methanol on the latticework structures was examined by STM and new bright features were observed after exposure to methanol at RT (Figure 6a). An apparent difference from the case of formic acid adsorption was the site of adsorbates with bright protrusions. Preferential adsorption of methanol on the center-bright spots on the narrow terraces was observed as shown in Figure 6b in comparison with Figure 6c for the image of the same area before methanol exposure. The new adsorbate stably existed even after annealing at 400 K, by which temperature molecularly adsorbed methanol should have desorbed as reported in TPD of methanol on TiO_2 surface.[25,35,36] Therefore, they can be assigned to methoxy species, formed by

$$CH_3OH(g) + O^{2-}(s) \rightarrow CH_3O^-(a) + OH^-(a) \qquad (2)$$

where O^{2-}(s) represents oxygen anion at the surface. The methoxy species did not form ordered structure by further exposure to methanol either. After further exposure to methanol, however, bright spots were also observed on side-bright spots. We tentatively assign them to methoxy species migrated from the center-bright spots because of repulsive interaction between methoxy species at higher coverage. These results indicate that the center-bright spot and the side-bright spot are different not only in topographic height but also in a chemical property on adsorption of molecules.

For comparison of an adsorption property, methanol adsorption on TiO_2(110) surface was also examined. No features assignable to stable adsorbates were observed even after exposure to 33 L of methanol at RT (data not shown). The result is quite different from that on the TiO_2(001) surface shown in Figure 6. It has been reported that the majority of methanol adsorbs molecularly on TiO_2(110) at RT.[35,37] STM images of TiO_2(110)−(1 × 1) became blurred soon after exposure to methanol and clear images gradually recovered after continuous scanning for ∼30 min. It may indicate that weakly bound methanol species were present on the surface but not imaged because of high mobility at RT.

Stability of the latticework structure against thermal reaction of adsorbed molecules was examined. Figure 7a (7b) shows an STM image of the latticework structure after exposure to 12 L of formic acid (48 L of methanol) at RT followed by annealing to 700 K. Previous TPD studies on the reactions of adsorbed formate and methoxy on TiO_2 surfaces indicated that they reacted and desorbed below 700 K.[12,24,25,35,36] Some particles were observed after formic acid reaction (Figure 7a). The size of the largest particle was 1.6 nm in height and 6.0 nm in diameter without correction of tip shape convolution. However, it was only 3.2% of the surface area and the latticework structure was maintained in 97% of the surface. The latticework structure entirely remained after methanol reaction (Figure 7b).

4. Discussion

4.1 Formation of the Latticework-Like Structure. The latticework structure observed by STM probably corresponds to the higher-temperature phase in the previous studies, judging from the LEED pattern, its dependency on the primary electron energy, and the similar treatment temperature.[18,25] The surface structure was homogeneous on the whole surface effective for STM measurements. Large-scale hill-like structure and particle-like structure were formed by annealing at the lower and higher temperatures in the order of 100 K, respectively.[28] We also observed that the stoichiometry of the TiO_2(001) substrate before annealing was important for preparing the lattice structure. Preferential sputtering of oxygen atoms and desorption of oxygen atoms during cleaning cycles gradually reduce the substrate. With a reduced substrate, the particle-like structure formed at the lower temperature close to that used in the present study, and the control of heating and cooling rates was important to prepare the ordered latticework structure. Similarly, the preparation temperature for TiO_2(110)−(1 × 2), which was slightly reduced surface phase,[30] is lowered by reduction of the

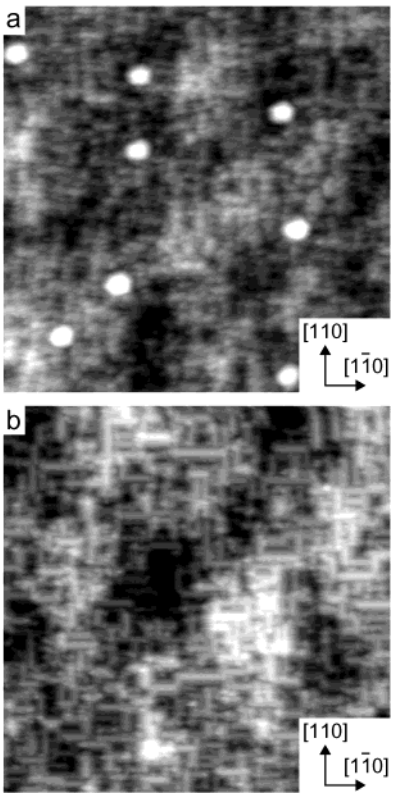

Figure 7. CCTs (80 × 80 nm^2) of a latticework structure on TiO_2-(001) after adsorption and thermal reaction of formic acid or methanol. The clean latticework structure was exposure to (a) 12 L of formic acid (V_s: +2.0 V, I_t: 0.05 nA) and (b) 48 L of methanol (V_s: +2.0 V, I_t: 0.03 nA) at RT, respectively, and annealed to 700 K. The surface structure is mostly preserved even after such thermal reactions while some protrusions were observed in (a) with a low density.

substrate. Thus, different degree of reduction of the substrate may be a reason the latticework structure was not observed in previous SPM studies.[19−22] In a recent STM observation of the ($7\sqrt{2} \times \sqrt{2}$) networklike structure on TiO_2(001), the surface was annealed above 1473 K with heating and cooling rates of ±100 K s^{-1}.[23] We suppose the substrate would have been highly reduced on such a treatment condition. Surface periodicity from the electron diffraction pattern and the characteristics of STM images of the surface are different from the latticework structure observed in the present study. Although there may be some similarity in local structure between the network structure and the latticework structure, we do not discuss the differences in detail here and concentrate on elucidating the atomic-scale surface structure of the stepped wide rows.

4.2 Atomic-Scale Structure of the Latticework Structure. Constant current topography measurements are affected not only by physical geometry but also by local electronic density of states of the tip and the sample. At a positive sample bias voltage (V_s) that we used for stable surface imaging of TiO_2(001) surfaces, the major path for tunneling electrons is from the Fermi energy of the tip to the unoccupied states of sample surface (the Fermi energy of the sample + eV_s).[38] Rutile TiO_2 bulk has a filled valence band of predominantly O 2p character and an empty conduction band of predominantly Ti 3d character, separated by a band gap of 3.1 eV.[1] The TiO_2(110) surface consists of alternating rows of 5-fold coordinated Ti rows at the troughs and bridging O rows at the ridges, which locate 0.11 nm above the underlying Ti−O plane. It has been established from an ab initio calculation that 5-fold coordinated Ti atoms are observed higher than the bridging oxygen atoms in constant current topography at positive sample bias voltages.[39] STM observation of selective adsorption of formic acid on 5-fold Ti sites also supported the conclusion.[30,31] Thus, preferential tunneling to unoccupied states with Ti 3d character overcomes the physical geometry. On WO_3(001) surface, which is also a d^0 metal oxide, it has been reported that physical geometry remained in STM images: on-top oxygen atoms were visible as bright spots even at positive sample bias voltages because significant mixing of W 5d state with O 2p state increased the unoccupied density of states at oxygen atoms.[40,41]

Formic acid dissociatively adsorbs on Ti cations of TiO_2 surfaces to form a formate ion at room temperature by eq 1. Thus, this molecule has played a crucial role as a probe to identify exposed Ti sites on TiO_2(110) by STM.[30,31] It is now established from experiments[30,31,42−44] and a theoretical calculation[34] that formate ions adsorb with a bridged configuration through two oxygen atoms of formate to two 5-fold coordinated Ti atoms with a 0.3-nm separation on TiO_2(110)−(1 × 1). Atom-resolved STM observations (Figure 3) revealed that the latticework structure consisted of narrow terraces separated by steps and each narrow terrace was covered with ordered bright spots as schematically shown in Figure 3d. Formate ions adsorbed on the sites corresponding to the bright spots of the substrate (Figure 5b). Therefore, we consider that the bright spots of the substrate can be assigned to coordinatively unsaturated Ti atoms. The bright protrusion of a formate ion observed by STM is probably due to electron tunneling to the lowest unoccupied molecular orbital (LUMO) localized at O−C−O.[31] Although it is difficult to determine the adsorption configuration by STM, formate ions on the latticework structure probably adsorb as unidentate or bidentate forms because the distance between two neighboring center-bright spots and between the center-bright spot and the side-bright spot, 0.65 and 0.50 nm, respectively, is too far from each other for a formate to form a bridge configuration.

The upper left side of Figure 8 shows a bulk-terminated {114}-faceted structure, which was previously proposed for the structure for the higher-temperature phase. A combination of {114}-microfacet with several step depths can reproduce the gross feature of the STM image in Figure 3, where row structures with narrow terraces separated by single-height steps are running along the [110] and the [1$\bar{1}$0] directions. However, the {114}-microfaceted model cannot reproduce the details of the atom-resolved STM image. In a unit cell surrounded by a rectangle, which is equivalent to that in Figure 3d, five Ti atoms are exposed: three 4-fold coordinated Ti atoms on the terrace and two 5-fold coordinated Ti atoms on the zigzag steps. Positions of the exposed Ti atoms in the unit cell are drawn at the top left of Figure 8. They are not consistent with the positions of the bright spots in Figure 3. In addition, if we compare the {114}-microfaceted model with a flat TiO_2(001) bulk-terminated surface, the density of 4-fold coordinated Ti atoms is lower but the total coordination number of exposed Ti atoms to O atoms per unit cell is the same (Table 1). Therefore, significant stabilization cannot be expected for the {114}-faceted model. Although large displacements of atom positions to reduce high surface energy of a bulk-truncated TiO_2(001) surface have been suggested by several theoretical calculations,[7,8,45,46] there is a distinct limitation to predict ion of the surface structure, which may be different from the bulk-truncated one in composition, by ab initio calculation at present. These results indicate that the atom-resolved STM images obtained here is a clue to construct a new structural model.

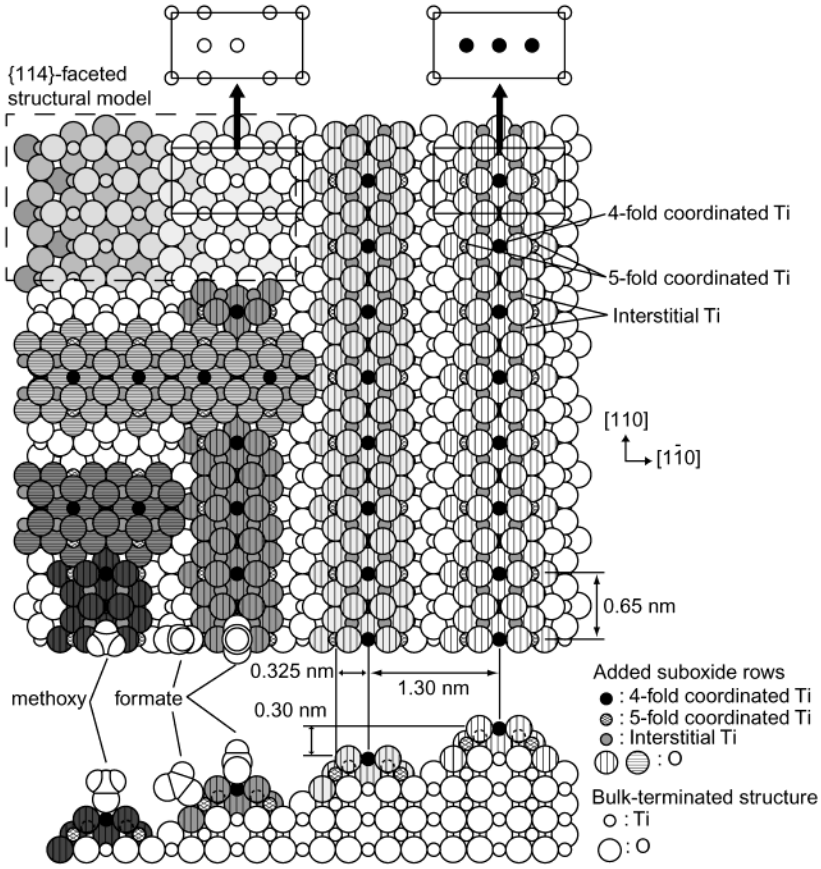

Figure 8. Structural model (top and side view) of the latticework structure on TiO_2(001). Suboxide rows are added on the bulk-terminated (1×1) structure. The added rows are crossed with one another at lower left region. Previously proposed {114}-faceted structural model is also displayed at the upper left for comparison. Positions of coordinatively unsaturated Ti atoms in a unit cell of the two structural models are picked up at the top of the figure. Small and large empty circles represent Ti and O atoms in a bulk crystal, respectively. Filled, shaded, and gray small circles represent 4-fold coordinated, 5-fold coordinated, and interstitial Ti atoms in the added suboxide rows, respectively. Shadings were used for the added rows and {114}-faceted region to clarify the height differences between them. Adsorbed formate and methoxy species are also drawn at lower left in the figure, where corresponding van der Waals spheres are postulated for each atom.

TABLE 1: Total Number of Unsaturated Ligand Coordination of Exposed Ti Atoms and the Number of 4-Fold and 5-Fold Coordinated Ti Atoms Per Unit Cell of a Bulk-Terminated {114}-Faceted Structure for Three Surface Structures as Barometers of Surface Stability

	number of exposed Ti atoms		total number of unsaturated coordination of exposed Ti atoms
	4-fold	5-fold	
bulk-terminated (001) structure	4	0	8
bulk-terminated {114}-faceted structure	3	2	8
latticework structure with added rows (Figure 8)	1	3	5

TiO_2 is a d^0 metal oxide and Ti cations hold the highest oxidation states. In reduced form, Ti_2O, TiO, Ti_2O_3, and Ti_3O_5 are well known as separate compounds. Besides these compounds, two series of Magnéli phase exist between TiO_2 and Ti_3O_5. Magnéli phases consist of slabs of the rutile structure separated by a regular array of crystallographic shear (CS) planes, in which certain lattice planes move relative to each other as a result of planar defect clustering leading to the collapse of the lattice. The {121} series with Ti_nO_{2n-1} ($4 < n < 10$) and the {132} series with Ti_nO_{2n-1} ($16 < n < \sim 37$) are formed and some of the CS planes that appeared on TiO_2(110) have been analyzed by STM.[47−49] Local structures of the compounds were examined if they fit to the narrow terrace of the latticework structure, but it failed. Although the {112} series CS planes[48] may form narrow terraces separated by single-height steps along the [110] and [1$\bar{1}$0] directions, the average plane of the slope is different from the latticework structure ({114} planes) and the shear process does not change the structure of each terrace from the bulk-terminated one.

At ternary oxide systems of Ti with Cr, Ga, Fe, and so forth, Ti cations diffuse into an empty octahedral void of oxygen anions at the first stage of the formation of CS planes.[50,51] We have previously proposed on the basis of STM observations that the Ti_2O_3 added row was formed on slightly reduced $TiO_2(110)-(1 \times 1)$ as a surface-limited phase.[9,14,30,52] In the Ti_2O_3 added-row model, Ti^{3+}'s are positioned at interstitial octahedral sites of oxygen atoms whose positions are assumed to be an extension of the substrate bulk. The model has been supported by the results of ESDIAD,[53] NC-AFM,[10,54] and a theoretical calculation.[55] We constructed a structural model for the latticework structure following the concept of Ti_2O_3 added row on TiO_2(110). We added a suboxide row on each narrow terrace of the {114}-microfaceted structure.

We constructed a model to reproduce the atom-resolved STM image in Figure 3 on the basis of several assumptions as follows:

(1) one exposed Ti atom corresponds to one bright spot in the STM image as discussed above;

(2) oxygen atoms are located at bulk-extended positions of the substrate and Ti atoms are located within reasonable distances from oxygen atoms (0.179−0.186 nm for Ti_2O_3 added row[55] and 0.194−0.197 nm for TiO_2 bulk) with preference to bulk-extended positions or interstitial positions of octahedral oxygen void;

(3) total coordination number of exposed Ti cations (five is the maximum for each exposed Ti cation) in a unit cell is as large as possible for surface stabilization; and

(4) O/Ti ratio is equal to or less than 2 because the surface is somewhat reduced after annealing to 1050 K under UHV.

A model of added-row structure is shown in Figure 8. A suboxide row, which contains four interstitial Ti^{3+} ($=Ti_4O_6$) and three exposed Ti^{4+} ($=Ti_3O_6$) per the unit cell, is added on narrow terraces of the {114}-microfaceted structure. Stoichiometry of the added suboxide row is Ti_7O_{12} ($=TiO_{1.71}$) at the top terrace and Ti_7O_{11} ($=TiO_{1.57}$) at other narrow terraces on the {114}-slopes of the stepped wide row. All the atoms in the added-row model hold bulk-extended positions except for the interstitial Ti atoms. Thus, the intersection of crossing rows observed in Figure 3 can be easily reproduced as shown in the left-hand side of Figure 8. A pyramidal structure in Figure 4 can also be reproduced. Positions of the exposed Ti atoms in the added-row model are schematically illustrated at the top right of Figure 8. We can safely assume that three exposed Ti atoms represented by black dots mainly contribute to electron tunneling at the top terrace because of a geometric reason. Therefore, the center-bright spots and the side-bright spots observed in Figure 3 probably correspond to 4-fold coordinated Ti atoms at the center of the row and 5-fold coordinated Ti atoms at both sides, respectively. The 5-fold coordinated Ti atoms that face to step edges on lower terraces are difficult to be resolved in STM images because of a finite radius tip apex. Thus, at narrow terraces on the slope of the stepped wide row, it is expected that two of the three exposed Ti atoms in the unit cell are mainly resolved by STM. These are consistent with the STM images shown in Figure 3. As shown in Table 1, the total number of unsaturated ligand coordination of exposed Ti atoms as well as the number of 4-fold coordinated Ti atoms per a unit cell are lower than those of the bulk-terminated TiO_2(001) and the bulk-terminated {114}-faceted model.

Formate ions adsorbed on the stepped wide row are schematically drawn at the lower part of Figure 8, tentatively assuming bidentate form for a center-bright spot (4-fold coordinated Ti) and unidentate form for a side-bright spot (5-fold coordinated Ti). However, we could not observe formate ions at sites on the side-bright spots that face to step edges on the lower terrace. At the step between the topmost terrace and the second terrace in Figure 8, local geometry of 5-fold coordinated Ti atoms of the added row on the second terrace and 5-fold coordinated Ti atoms of the bulk-terminated structure are almost the same. If a formate ion is placed on these sites in a unidentate or bidentate form, the {111}-slope of the added-row facing across the trough is close to overlap the van der Waals spheres of O atoms or a C atom of the formate ion. Thus, adsorption of formic acid on these sites seems to be difficult because of steric blocking even if these Ti atoms are coordinatively unsaturated.

Although the periodicity of the added-row model along the row axis (0.65 nm) coincides with STM images, the distance between a 4-fold coordinated Ti atom and a neighboring 5-fold coordinated Ti atom (0.325 nm) is smaller than the observed value (∼0.5 nm). Height difference between the 4-fold coordinated Ti atom and the neighboring 5-fold coordinated Ti atom in the model is 0.15 nm, which is slightly larger than the observed value of 0.05 nm (Figure 3b). The bulk-extended positions are assumed for most of the atoms in the added-row model. The observed structure may be somewhat relaxed from the model perpendicular to the row axis because of the presence of interstitial Ti atoms. Such relaxation makes the discrepancies smaller, but we did not dare to relax the model without any substantial information. Besides, the difference in the direction parallel to the surface may be explained by the direction of an orbital extended from the unsaturated Ti atoms. On a Si(111)−(3 × 2) reconstructed surface, characteristic pentagonal group of spots has been observed in STM images at a positive sample bias voltage and was assigned to dangling bond states of five-membered Si rings.[56−58] A theoretical calculation on its optimum surface structure and STM image expected from the structure revealed that pentagonal bright spots in the STM image deviated outside of the five-membered Si ring by 0.08−0.18 nm because of tilt of the dangling bonds from the surface normal. In the present study, an empty state lobe of the 5-fold coordinated Ti atom on the added row can be expected to extend normal to the slope of the added row. Therefore, it may be possible that the tilted empty state lobe at the 5-fold coordinated Ti atom in the added row caused bright spots at larger separation from the 4-fold coordinated Ti atom than the geometric separation in the model.

Methanol adsorption on the latticework structure indicated that the center-bright spot (4-fold coordinated Ti atom in Figure 8) and the side-bright spot (5-fold coordinated Ti atom in Figure 8) differ not only in topographic height but also in a chemical property on dissociative adsorption of methanol. Methanol preferentially adsorbed on the 4-fold coordinated Ti atoms as methoxy species (Figure 6). Dissociative adsorption process of eq 2 involves two substrate atoms (Ti and O). A surface oxygen atom withdraws proton from CH_3OH to form surface hydroxyl. It suggests that local geometry and electronic states of a neighboring O atom are also important for the process. However, there is always neighboring oxygen atoms with similar unsaturated coordination and similar distance for both kinds of Ti atoms. Therefore, we consider that the difference in chemical property can be attributed to the difference in coordination number of Ti cation. On TiO_2(110) surface, which contains only 5-fold coordinated Ti atoms, the majority of methanol adsorbed molecularly at RT.[35,37] Our STM measurements on TiO_2(110) supported this view.

The added-row model in Figure 8 seems to be an appropriate model that is consistent with the atom-resolved STM images of the surface and molecule-adsorbed STM images. It also has a reasonable stoichiometry and local coordination around each atoms. For further elucidation of the structures, NC-AFM measurements for protruding oxygen atoms, which cannot be observed by STM,[10] medium energy ion scattering spectroscopy, and theoretical calculations with a rather large system would be helpful.

4.3 Latticework Structure as a Reaction Field. Stability of a surface structure against adsorption and reaction of adsorbed molecules is an important issue particularly for catalytic reactions on the surface. Neither large displacement of atoms nor reconstruction of the latticework structure on TiO_2(001) was observed after the adsorption of formic acid and methanol as shown in Figures 5 and 6. Particularly for methanol, no structural change was observed even after repeated cycles of adsorption and reaction by annealing to 700 K (surface after a cycle is shown in Figure 7b). In formic acid, some protrusions with unknown composition were formed after the thermal reaction (Figure 7a), though the density of the protrusions was small

enough. Repeated cycles of adsorption and reaction increased the density of such protrusions. Precise analyses of reaction products are necessary to discuss the details, but we assume that a change in local stoichiometry caused formation of such protrusions. Addition of oxygen atoms from formate to the added row may lead to reaction with Ti cations diffused from bulk interstitials to the surface. Actually, formation of TiO_x by oxidation of such Ti cations has been confirmed by STM.[14−16] Except for such minor reaction, stability of the latticework structure on TiO_2(001) is rather high in contrast to the bulk-terminated structure. It can be expected that this surface works as an effective reaction field in a catalytic reaction system as partly shown in effective adsorption ability of methanol as methoxy species.

5. Summary

Surface structure of the rutile TiO_2(001) was examined by STM on the atomic scale. After annealing to 1050 K under ultrahigh vacuum after Ar^+-sputtering, the latticework structure that consisted of atomically ordered stepped wide rows such as "bleachers" running along the [110] and [1$\bar{1}$0] directions were observed. This surface was assigned to the higher-temperature phase reported in previous LEED studies. On the basis of atom-resolved STM images as well as local coordination considerations, we proposed an added-row structural model, which consists of Ti_7O_{12} suboxide row added on each narrow terrace of a {114}-microfacet structure. The added row contained 4-fold coordinated and 5-fold coordinated Ti atoms, each of which was observed as bright spot in the STM images and formic acid adsorbed on each site. Preferential adsorption of methanol on the specific sites supported the assignment of the two kinds of exposed Ti.

Acknowledgment. This study was supported by a Grant-in-aid for The 21st Century COE Program for Frontiers in Fundamental Chemistry from the Ministry of Education, Culture, Sports, Science, and Technology.

References and Notes

(1) Henrich, V. E.; Cox, P. A. *The Surface Science of Metal Oxides*; Cambridge University Press: Cambridge, U.K., 1996.
(2) Iwasawa, Y. *Stud. Surf. Sci. Catal.* **1996**, *101*, 21.
(3) Lai, X.; Clair, T. P. S.; Valden, M.; Goodman, D. W. *Prog. Surf. Sci.* **1998**, *59*, 25.
(4) Diebold, U. In *Chem. Phys. Solid Surf.*; King, D. A., Woodruff, D. P., Eds.; Elsevier: Amsterdam, 2001; Vol. 9, p 443.
(5) Maschhoff, B. L.; Pan, J. M.; Madey, T. E. *Surf. Sci.* **1991**, *259*, 190.
(6) Charlton, G.; Howes, P. B.; Nicklin, C. L.; Steadman, P.; Taylor, J. S. G.; Muryn, C. A.; Harte, S. P.; Mercer, J.; McGrath, R.; Norman, D.; Turner, T. S.; Thornton, G. *Phys. Rev. Lett.* **1997**, *78*, 495.
(7) Ramamoorthy, M.; Vanderbilt, D.; King-Smith, R. D. *Phys. Rev. B* **1994**, *49*, 16721.
(8) Muscat, J.; Harrison, N. M. *Surf. Sci.* **2000**, *446*, 119.
(9) Onishi, H.; Iwasawa, Y. *Surf. Sci.* **1994**, *313*, L783.
(10) Fukui, K.; Onishi, H.; Iwasawa, Y. *Phys. Rev. Lett.* **1997**, *79*, 4202.
(11) Iwasawa, Y.; Onishi, H.; Fukui, K. *Top. Catal.* **2001**, *14*, 163.
(12) Onishi, H.; Aruga, T.; Iwasawa, Y. *J. Catal.* **1994**, *146*, 557.
(13) Onishi, H.; Yamaguchi, Y.; Fukui, K.; Iwasawa, Y. *J. Phys. Chem.* **1996**, *100*, 9582.
(14) Onishi, H.; Iwasawa, Y. *Phys. Rev. Lett.* **1996**, *76*, 791.
(15) Bennett, R. A.; Stone, P.; Price, N. J.; Bowker, M. *Phys. Rev. Lett.* **1999**, *82*, 3831.
(16) Li, M.; Hebenstreit, W.; Gross, L.; Diebold, U.; Henderson, M. A.; Jennison, D. R.; Schultz, P. A.; Sears, M. P. *Surf. Sci.* **1999**, *437*, 173.
(17) Tait, R. H.; Kasowski, R. V. *Phys. Rev. B* **1979**, *20*, 5178.
(18) Firment, L. E. *Surf. Sci.* **1982**, *116*, 205.
(19) Poirier, G. E.; Hance, B. K.; White, J. M. *J. Vac. Sci. Technol., B* **1992**, *10*, 6.
(20) Watson, B. A.; Barteau, M. A. *Chem. Mater.* **1994**, *6*, 771.
(21) Nörenberg, H.; Dinelli, F.; Briggs, G. A. D. *Surf. Sci.* **2000**, *446*, L83.
(22) Antonik, M. D.; Edwards, J. C.; Lad, R. J. *Mater. Res. Soc. Symp. Proc.* **1992**, *237*, 459.
(23) Nörenberg, H.; Dinelli, F.; Briggs, G. A. D. *Surf. Sci.* **1999**, *436*, L635.
(24) Kim, K. S.; Barteau, M. A. *Langmuir* **1990**, *6*, 1485.
(25) Kim, K. S.; Barteau, M. A. *Surf. Sci.* **1989**, *223*, 13.
(26) Kim, K. S.; Barteau, M. A. *J. Catal.* **1990**, *125*, 353.
(27) Barteau, M. A. *Chem. Rev.* **1996**, *96*, 1413.
(28) Fukui, K.; Tero, R.; Iwasawa, Y. *Jpn. J. Appl. Phys.* **2001**, *40*, 4331.
(29) Iwasawa, Y. *Surf. Sci.* **1998**, *404*−*404*, 8.
(30) Onishi, H.; Fukui, K.; Iwasawa, Y. *Bull. Chem. Soc. Jpn.* **1995**, *68*, 2447.
(31) Onishi, H.; Iwasawa, Y. *Chem. Phys. Lett.* **1994**, *226*, 111.
(32) Uetsuka, H.; Sasahara, A.; Onishi, H. *Jpn. J. Appl. Phys.* **2000**, *39*, 3769.
(33) Tanner, R. E.; Sasahara, A.; Liang, Y.; Altman, E. I.; Onishi, H. *J. Phys. Chem. B* **2002**, *106*, 8211.
(34) Käckell, P.; Terakura, K. *Surf. Sci.* **2000**, *461*, 191.
(35) Henderson, M. A.; Otero-Tapia, S.; Castro, M. E. *Faraday Discuss.* **1999**, *114*, 313.
(36) Román, E.; Bustillo, F. J.; de Segovia, J. L. *Vacuum* **1990**, *41*, 40.
(37) Onishi, H.; Aruga, T.; Egawa, C.; Iwasawa, Y. *Surf. Sci.* **1988**, *193*, 33.
(38) Wiesendanger, R. *Scanning Probe Microscopy and Spectroscopy: Methods and Applications*; Cambridge University Press: New York, 1994.
(39) Diebold, U.; Anderson, J. F.; Ng, K.-O.; Vanderbilt, D. *Phys. Rev. Lett.* **1996**, *77*, 1322.
(40) Jones, F. H.; Rawlings, K.; Foord, J. S.; Cox, P. A.; Egdell, R. G.; Pethica, J. B.; Wanklyn, B. M. R. *Phys. Rev. B* **1995**, *52*, R14392.
(41) Tanner, R. E.; Meethunkij, P.; Altman, E. I. *J. Phys. Chem. B* **2000**, *104*, 12315.
(42) Fukui, K.; Onishi, H.; Iwasawa, Y. *Chem. Phys. Lett.* **1997**, *280*, 296.
(43) Chambers, S. A.; Thevuthasan, S.; Kim, Y. J.; Herman, G. S.; Wang, Z.; Tober, E.; Ynzunza, R.; Morais, J.; Peden, C. H. F.; Ferris, K.; Fadley, C. S. *Chem. Phys. Lett.* **1997**, *267*, 51.
(44) Guo, Q.; Cocks, I.; Williams, E. M. *J. Chem. Phys.* **1997**, *106*, 2924.
(45) Yin, X.; Miura, R.; Endou, A.; Gunji, I.; Yamauchi, R.; Kubo, M.; Stirling, A.; Fahmi, A.; Miyamoto, A. *Appl. Surf. Sci.* **1997**, *119*, 199.
(46) Schelling, P. K.; Yu, N.; Halley, J. W. *Phys. Rev. B* **1998**, *58*, 1279.
(47) Rohrer, G. S.; Henrich, V. E.; Bonnell, D. A. *Science* **1990**, *250*, 1239.
(48) Nörenberg, H.; Tanner, R. E.; Schierbaum, K. D.; Fischer, S.; Briggs, G. A. D. *Surf. Sci.* **1998**, *396*, 52.
(49) Bennett, R. A.; Poulston, S.; Stone, P.; Bowker, M. *Phys. Rev. B* **1999**, *59*, 10341.
(50) Hyde, B. G.; Andersson, S. *Inorganic Crystal Structures*; Wiley-Interscience: New York, 1989.
(51) Hyde, B. G.; Bagshaw, A. N.; Andersson, S.; O'Keeffe, M. *Annu. Rev. Mater. Sci.* **1974**, *4*, 43.
(52) Takakusagi, S.; Fukui, K.; Nariyuki, F.; Iwasawa, Y. *Surf. Sci.* **2003**, *523*, L41.
(53) Guo, Q.; Cocks, I.; Williams, E. M. *Phys. Rev. Lett.* **1996**, *77*, 3851.
(54) Ashino, M.; Sugawara, Y.; Morita, S.; Ishikawa, M. *Phys. Rev. Lett.* **2001**, *86*, 4334.
(55) Ng, K.-O.; Vanderbilt, D. *Phys. Rev. B* **1997**, *56*, 10544.
(56) Sakama, H.; Kunimatsu, D.; Kageshima, M.; Kawazu, A. *Phys. Rev. B* **1996**, *53*, 6927.
(57) Dabrowski, J.; Müssig, H.-J.; Wolff, G. *Surf. Sci.* **1995**, *331*−*333*, 1022.
(58) Dabrowski, J.; Müssig, H.-J.; Wolff, G. *Phys. Rev. Lett.* **1994**, *73*, 1660.